Crystal Structure of the Lytic Transglycosylase from Bacteriophage Lambda in Complex with Hexa-*N*-acetylchitohexaose[†,‡]

Adelaine K.-W. Leung,[§] Henry S. Duewel,[||] John F. Honek,[||] and Albert M. Berghuis*[,§]

Antimicrobial Research Centre and Department of Biochemistry, McMaster University, Hamilton, Ontario L8N 3Z5, Canada, and Department of Chemistry, University of Waterloo, Waterloo, Ontario N2L 3G1, Canada

Received December 11, 2000; Revised Manuscript Received March 8, 2001

ABSTRACT: The three-dimensional structure of the lytic transglycosylase from bacteriophage lambda, also known as bacteriophage lambda lysozyme, complexed to the hexasaccharide inhibitor, hexa-*N*-acetylchitohexaose, has been determined by X-ray crystallography at 2.6 Å resolution. The unit cell contains two molecules of the lytic transglycosylase with two hexasaccharides bound. Each enzyme molecule is found to interact with four *N*-acetylglucosamine units from one hexasaccharide (subsites A−D) and two *N*-acetylglucosamine units from the second hexasaccharide (subsites E and F), resulting in all six subsites of the active site of this enzyme being filled. This crystallographic structure, therefore, represents the first example of a lysozyme in which all subsites are occupied, and detailed protein−oligosaccharide interactions are now available for this bacteriophage lytic transglycosylase. Examination of the active site furthermore reveals that of the two residues that have been implicated in the reaction mechanism of most other c-type lysozymes (Glu35 and Asp52 in hen egg white lysozyme), only a homologous Glu residue is present. The lambda lytic transglycosylase is therefore functionally closely related to the *Escherichia coli* Slt70 and Slt35 lytic transglycosylases and goose egg white lysozyme which also lack the catalytic aspartic acid.

Lysozymes are widely distributed in nature and function to cleave the glycan chains of the bacterial peptidoglycan between *N*-acetylmuramic acid (MurNAc)[1] and *N*-acetylglucosamine (GlcNAc) residues (*1*, *2*). The lysozyme from bacteriophage lambda [lambda lysozyme (LaL)] is the late gene product of the lambda *R* gene (*3*−*5*). Unlike other lysozymes, however, this enzyme does not produce a reducing end upon cleavage of the peptidoglycan but rather utilizes the 6-OH of the same MurNAc residue to produce a 1,6-anhydromuramic acid terminal residue (*6*). Hence, the bacteriophage lambda lysozyme is a lytic transglycosylase. An identical 1,6-anhydro bond is formed in bacterial peptidoglycan by the action of the lytic transglycosylases from *Escherichia coli.* One soluble (Slt70) and five membrane-bound (MltA−D and EmtA) lytic transglycosylases have been identified in *E. coli*, and homologous genes have been identified in many other bacteria (*7*−*16*). A number of important physiological roles have been suggested for these bacterial lytic transglycosylases and include peptidoglycan construction and renovation as well as bacterial pore creation (*2*, *16*, *17*).

In addition to the obvious mechanistic concerns as to how these enzymes accomplish the transglycosylation reaction compared to the hydrolytic reaction catalyzed by "standard" lysozymes, the 1,6-anhydro-containing peptidoglycan fragments themselves have generated much interest. The etiological agent of whooping cough, *Bordetella pertussis*, releases *N*-acetylglucosaminyl-1,6-anhydro-*N*-acetylmuramyl-L-alanyl-γ-D-glutamyl-*meso*-diaminopimelyl-D-alanine. This 1,6-anhydro muropeptide produces the same specific cell damage observed in the respiratory tract during infection by *B. pertussis* (*18*). Other physiological responses observed with these fragments include somnogenic (*19*, *20*), arthritogenic (*21*), and pyrogenic (*22*) activites. In addition, interleukin-1β, interleukin-6 (*23*), and granulocyte colony-stimulating factor expression (*24*) in human monocytes are induced by 1,6-anhydro muropeptides. These muropeptides have also been shown to suppress appetite and weight gain in mammals (*25*). Given the possibly numerous applications for 1,6-anhydro muropeptides, attempts have been made to immobilize lytic transglycosylases from *E. coli* to increase production of these compounds (*9*).

The crystal structures of the *E. coli* Slt70 and Slt35 (a proteolytic fragment of the membrane-bound MltB) lytic transglycosylases have been previously determined (*26*, *27*).

[†] This work was supported by the Natural Sciences and Engineering Research Council of Canada (J.F.H.) and the Canadian Institutes for Health Research (A.M.B.). A.M.B. is the recipient of a CIHR/PMAC-HRF Research Career Award. H.S.D. was a recipient of an NSERC postgraduate scholarship.

[‡] The atomic coordinates of the bacteriophage lambda lytic transglycosylase complexed with hexa-*N*-acetylchitohexaose have been deposited in the Protein Data Bank (entry 1D9U).

* To whom correspondence should be addressed. E-mail: berghuis@mcmaster.ca. Telephone: (905) 525-9140, ext 22316. Fax: (905) 522-9033.

[§] McMaster University.

[||] University of Waterloo.

[1] Abbreviations: EDC, 1-ethyl-3-[3-(dimethylamino)propyl]carbodiimide; GEWL, goose egg white lysozyme; GlcNAc, 2-acetamido-2-deoxy-D-glucosamine (*N*-acetylglucosamine); $(GlcNAc)_6$, $\beta(1\rightarrow4)$-linked hexamer of 2-acetamido-2-deoxy-D-glucosamine (*N*-acetylglucosamine); HEWL, hen egg white lysozyme; LaL, bacteriophage lambda lysozyme/lytic transglycosylase; LaL·$(GlcNAc)_6$, LaL complexed with $(GlcNAc)_6$; mLaL, lambda lysozyme with tryptophan residues replaced with 7-azatryptophan; MurNAc, *N*-acetylmuramic acid; rmsd, root-mean-square deviation; PEG 2000 MME, polyethylene glycol 2000 monomethyl ether.

10.1021/bi0028035 CCC: $20.00
Published on Web 04/18/2001

Recently, additional structures have been determined with peptidoglycan fragments cocrystallized in the active site of these two enzymes (*28*, *29*). These studies have helped elucidate the molecular interactions between the oligosaccharide and enzyme, and have helped to define the number and location of each saccharide subsite in each lytic transglycosylase. Although the determination of the crystal structure of the bacteriophage lambda lytic transglycosylase has remained enigmatic, a derivative of LaL (mLaL for modified LaL) wherein all tryptophan residues have been replaced with 7-azatryptophan has allowed for the formation of crystals suitable for successful structure determination (*30*, *31*). However, to date, no structure has been determined for a cocrystal of LaL with a saccharide, preventing the elucidation of the exact nature of the saccharide−protein interaction for this phage lytic transglycosylase and of the detailed conformational changes that occur in LaL upon saccharide binding.

Herein, we report our recent success in the determination of the crystal structure of an oligosaccharide−bacteriophage lytic transglycosylase complex which now allows for the elucidation of the precise molecular interactions between the saccharide and wild-type phage enzyme. Fortuitously, the structure that has been determined contains *N*-acetylglucosamine units in all of the six subsites of the enzyme. Until now, the only structure of a lysozyme which contained six saccharide units was that of human lysozyme determined by Song and co-workers (*32*). However, in the human lysozyme−oligosaccharide complex, subsites E and F are actually empty and the two saccharide units are only bound close to these two subsites. Thus, our results finally provide a detailed view of this complex. In addition, the structure of the oligosaccharide−bacteriophage lytic transglycosylase complex also sheds light on the structural basis for this enzyme catalyzing a transglycosylation instead of a hydrolysis reaction.

EXPERIMENTAL PROCEDURES

Materials. All materials used were of the highest grade commercially available and were used without further purification. Oligosaccharides of GlcNAc were purchased from Siekagaku America, Inc. (Rockville, MD). 1-Ethyl-3-[3-(dimethylamino)propyl]carbodiimide (EDC) was from Sigma. Polyethylene glycol 2000 monomethyl ether (PEG 2000 MME) was purchased from Fluka. Recombinant LaL used for the chemical modification and crystallization experiments was obtained according to procedures previously described (*33*, *34*).

Chemical Modification. In a typical experiment, LaL (90 μM) was incubated in the presence of 25−100 mM EDC in 100 mM MES (pH 5.8) at 23 °C for various times. Identical controls lacking the modifying agent were also prepared. At various time intervals, aliquots (2 μL) were diluted with 998 μL of stabilizing buffer [100 mM potassium phosphate (pH 7.0), 0.5 M KCl, and 20% (v/v) glycerol]. Immediately following dilution of the aliquots, an aliquot from the diluted sample (4 μL) was assayed using the turbidimetric assay as described previously (*33*). The background level of lysis of the substrate cells (blank) was determined using only stabilizing buffer. Protection of LaL from EDC-mediated inactivation by $(GlcNAc)_n$ was achieved by inclusion of the required amount of solid $(GlcNAc)_n$ to the desired concentration with the samples.

Crystallization. On the basis of the results of the chemical modification experiments, possible crystallization conditions for LaL·$(GlcNAc)_n$ ($n = 4-6$) complexes were surveyed by the hanging drop vapor diffusion technique using a commercially available sparse matrix screening procedure (*35*, *36*; Hampton Research). While several promising conditions were found in this manner, crystals thus obtained suffered from severe twinning. Further refinement of crystal growth conditions (e.g., alterations in precipitant concentration, pH of the buffer, and/or additives) did not dramatically improve the quality of the crystals. However, the twinning could be reduced to acceptable levels (i.e., separation between split reflections was less than 1.5°) when using a microdialysis crystallization procedure. Therefore, crystals suitable for X-ray crystallographic analysis were obtained by preincubating a concentrated solution of LaL (10 mg/mL) in the presence of a 5-fold molar excess of $(GlcNAc)_6$; 5 μL of this protein solution was then deposited in the depression of a microdialysis button (Hampton Research) and sealed with a dialysis membrane. This microdialysis button was subsequently immersed in a solution containing 0.1 M sodium acetate (pH 4.6), 0.1 M ammonium sulfate, and 20% (w/v) PEG 2000 MME and allowed to equilibrate. Using this procedure, crystals grew within 1 week to an average size of 0.5 mm × 0.2 mm × 0.2 mm.

Data Collection and Processing. A nearly complete 2.6 Å resolution data set was collected from one single crystal on a Rigaku Raxis IIC area detector mounted on a Rigaku RU200 rotating anode operating at 50 kV and 60 mA, and equipped with Supper double focusing mirrors. To prevent decay, the crystal was flash-frozen and data collection was performed at an ambient temperature of −170 °C. Processing of the diffraction images was performed using the Denzo/Scalepack software package (*37*). Analysis of the diffraction images revealed that the LaL·$(GlcNAc)_6$ crystal belonged to orthorhombic space group $P2_12_12_1$ with the following cell dimensions: $a = 57.3$ Å, $b = 61.1$ Å, and $c = 122.5$ Å. Given this information, and the molecular weight of the protein, it was deduced that the crystallographic asymmetric unit contained two protein molecules (*38*). The mosaicity of the measured reflections was relatively large (1.2°); however, this was a direct consequence of the minor twinning present in the crystal. Pertinent statistics related to data processing are given in Table 1.

Structure Determination and Refinement. The structure of the LaL·$(GlcNAc)_6$ complex was determined by molecular replacement with X-PLOR (*39*), using the coordinates of the mLaL enzyme (*30*) (PDB entry 1AM7). Two solutions from the rotation search, corresponding to the orientations of the two molecules in the asymmetric unit, were readily found. The translation search also gave unequivocal solutions which agreed with reasonable packing constraints. Subsequently, reciprocal space restrained refinement of the structure and periodic real space inspection along with manual intervention were performed with X-PLOR and O, respectively (*39*, *40*). At the start of the refinement process, electron density for the $(GlcNAc)_6$ inhibitor could be identified in the active site of each LaL molecule in the asymmetric unit (Figure 1). However, a cautious approach was taken when modeling the sugar moieties into the density, and only gradually were

Table 1: Data Processing and Structure Refinement Statistics

resolution (Å)	4.0−2.6	2.7−2.6
completeness (%)	92.0	55.3
redundancy	7.7	1.2
R_{merge} (%)[a]	11.8	50.7
no. of atoms		
protein	2450	
$(GlcNAc)_6$	170	
sulfate ion	20	
solvent	31	
average temperature factor (Å^2)		
protein monomer A	29	
protein monomer B	31	
$(GlcNAc)_6$ molecule I	23	
$(GlcNAc)_6$ molecule II	36	
rmsd from ideality		
bond lengths (Å)	0.005	
bond angles (deg)	1.2	

	$F/\sigma F = 0$	$F/\sigma F = 2$	$F/\sigma F = 2$
no. of reflections	11803	10883	9906
completeness (%)	92.0	84.3	76.7
R-factor (%)[b]	23.2	21.4	20.7
R_{free} (%)[c]	30.4	28.6	27.8

[a] $R_{merge} = 100 \times \sum|I_i - \langle I\rangle|/\sum|I_i|$, where I_i is the observed intensity and $\langle I\rangle$ is the average intensity calculated from multiple observations. [b] *R*-factor $= 100 \times \sum|F_o - F_c|/\sum|F_o|$, where F_o and F_c are the observed and calculated structure factor amplitudes, respectively. [c] R_{free} is an *R*-factor which was calculated using 10% of the data, chosen randomly and omitted from refinement.

individual *N*-acetylglucosamine groups added to the structure. During the initial stages of refinement, four loop regions were also deleted from the model, based on poor agreement with sigma-A weighted electron density maps (*41*). These four regions were residues 55−60 and 129−138 in the two LaL molecules. As refinement progressed, these residues were added back into the model, albeit in a differing conformation. After the protein and inhibitor structures were essentially completed, a limited number of ordered solvent molecules were modeled. The criteria used for inclusion of solvent molecules were the presence of electron density upon visual inspection (in both sigma-A weighted $F_o - F_c$ and $2F_o - F_c$ maps), refinement of thermal factors to reasonable values, formation of stereochemically acceptable hydrogen bonding interactions, and no increase in R_{free} (to avoid overfitting during refinement of the structure; see Table 1). On the basis of thermal factors, the chemical environment, and the composition of the crystallization solution, four of these solvent molecules were afterward identified as sulfate ions, and thus so modeled. Refinement of the model was concluded when addition of solvent molecules and/or further refinement resulted in an increase in R_{free} (*42*). This final model is in good agreement with experimental data, as judged by the *R*-factor and R_{free} values, and displays excellent stereochemistry as evaluated by the program PROCHECK (*43*); e.g., 88.3% of the residues occupy the most favored regions of the Ramachandran plot, and none are in generously allowed or disallowed regions. Detailed statistics pertaining to the final model are given in Table 1.

RESULTS

Chitooligosaccharide Protection of Carboxyl Modification. Previous investigations utilizing differential scanning calorimetry, ^{1}H, ^{13}C, and ^{19}F nuclear magnetic resonance, and inhibition of bacterial lysis by LaL have shown that chitooligosaccharides can interact with LaL (*33*, *34*, *44*). Additional evidence for active site binding was sought prior to crystallization attempts. The involvement of carboxyl groups in the catalytic mechanism of LaL was investigated with the carboxyl group-specific water-soluble carbodiimide EDC (*45*). LaL was incubated with the reagent at pH 5.8 in the absence of an added nucleophile, and residual activity over time was determined by monitoring the bacteriolytic activity of LaL using the turbidimetric assay described previously (*33*). EDC resulted in time- and dose-dependent inactivation of LaL. Semilogarithmic plots of the time course of inactivation of LaL by various concentrations of EDC (ranging between 25 and 100 mM) were linear, indicating that the inactivation obeys pseudo-first-order kinetics (data not shown). A second-order rate constant of 0.33 M^{-1} min^{-1} was determined from a plot of the pseudo-first-order rate constants (k_{obs}) versus EDC concentration (not shown). The order of inactivation with respect to EDC concentration was determined by the method of Levy et al. (*46*) to be 1.2. The results indicate that an average of one molecule of carbodiimide binds to one molecule of LaL to effect inactivation and, because of the enhanced reactivity with carboxyl groups, suggest the possibility that a key Glu or Asp residue is being modified which results in enzyme inactivation.

To determine if the carboxyl groups modified by EDC are located in the active site of LaL, modifications were also performed in the presence of chitooligosaccharides. The effect of oligosaccharide protection on LaL inactivation by EDC is illustrated in Figure 2. The di- and trisaccharides were equally and only minimally effective in preventing inactivation by EDC. Under the conditions that were examined, the values of k_{obs} in the presence of 20 mM $(GlcNAc)_2$ and $(GlcNAc)_3$ are $\sim 1.25 \times 10^{-2}$ min^{-1}, which represents only a 20% reduction relative to the k_{obs} determined in the presence of 50 mM EDC only (1.58×10^{-2} min^{-1}). However, a substantial improvement in protection was observed when inactivation was conducted in the presence of 20 mM $(GlcNAc)_4$ ($k_{obs} \sim 0.10 \times 10^{-2}$ min^{-1}) or $(GlcNAc)_5$ ($k_{obs} \sim 0.05 \times 10^{-2}$ min^{-1}), the rate of inactivation decreasing by approximately 95% in the presence of each. Therefore, the tetra- and pentasaccharide, either directly or indirectly by inducing conformational changes, prevent the access of EDC to a particular region(s) of the enzyme in which are located one or more specific acidic residues that are important for the enzyme's bacteriolytic activity. As indicated by the selective protection, part of this binding region, which is not occupied by $(GlcNAc)_3$ but is with $(GlcNAc)_4$ and higher oligomers, appears to contain a functionally important glutamyl or aspartyl residue. The involvement of Glu19 in the mechanism of LaL has been implicated by mutations at this position (*47*). If it is assumed that Glu19 acts as the general acid, then, in analogy to Glu35 in hen egg white lysozyme (HEWL) and other glycosylases, this group should have an elevated pK_a to fulfill this role (*48*). The observed order of inactivation by EDC of 1.2 reflects possible modification primarily of this assumed catalytic general acid. These solution results are entirely compatible with the overall binding interactions seen in the crystal structure of the LaL·$(GlcNAc)_6$ complex (see below).

Overall Structure of the LaL·(GlcNAc)$_6$ Complex. The LaL·$(GlcNAc)_6$ complex crystallizes with two molecules per asymmetric unit in space group $P2_12_12_1$ (Figure 1). The

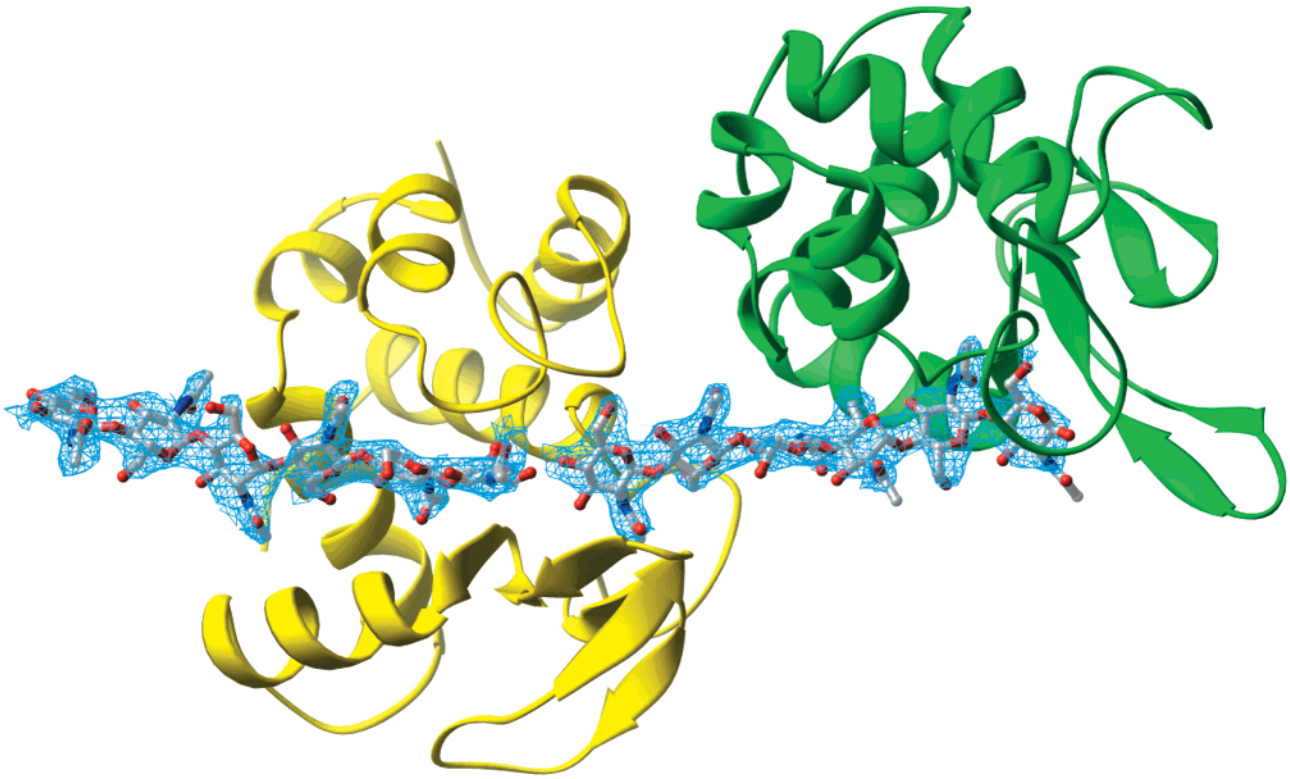

FIGURE 1: Electron density map for the hexasaccharide. Shown is the $2F_o - F_c$ electron density prior to modeling in the two hexa-*N*-acetylchitohexaose moieties and contoured at 1.0σ. Superimposed on the electron density map is also shown the final refined hexasaccharides and a Ribbons representation of the two LaL monomers present in the asymmetric unit. This figure was produced using Ribbons (*54*).

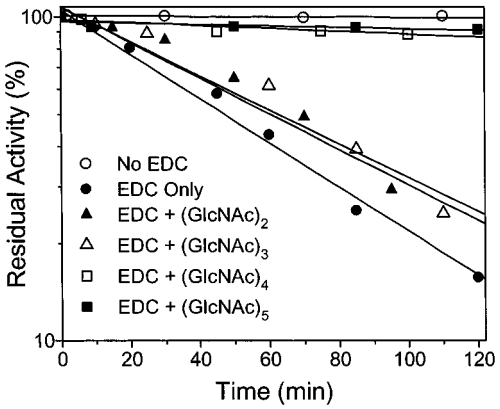

FIGURE 2: Protection of LaL from EDC inactivation by $(GlcNAc)_n$. LaL (1.6 mg/mL) was treated with EDC (50 mM) in the absence and presence of 20 mM $(GlcNAc)_n$ as indicated in 100 mM MES (pH 5.8). At the indicated times, samples were removed from the reaction mixtures, diluted with stabilizing buffer, and immediately assayed for residual activity.

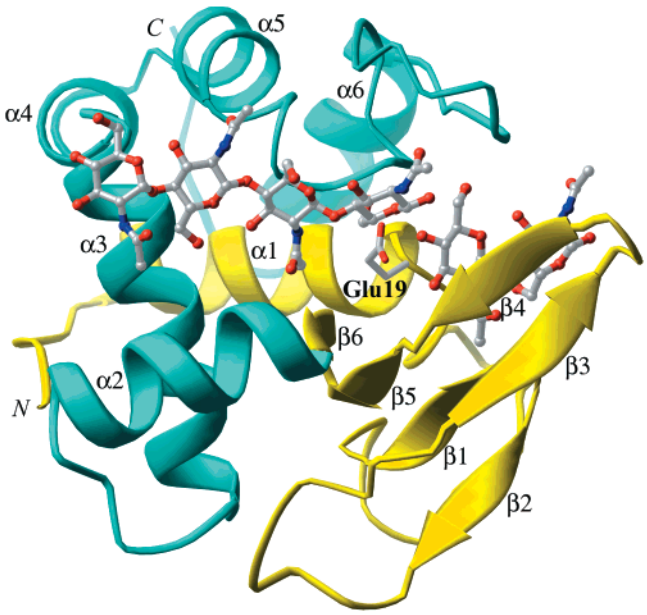

FIGURE 3: Domain structure of the LaL (monomer). In this schematic Ribbons diagram, the upper domain is shown in aqua and the lower domain of the protein in yellow. Furthermore, secondary structure elements are labeled and the catalytic glutamate is shown. Also displayed are the saccharide moieties of the two $(GlcNAc)_6$ molecules which bind to the LaL monomer. This figure was produced using Ribbons (*54*).

backbones of the two molecules, A and B, are similar with an rmsd of 0.39 Å (616 atoms used in the calculation). The main deviations are located in the loop regions on the protein surface. Also, the thermal factors for both molecules are similar, suggesting that conformational artifacts due to crystal packing interactions are likely absent.

LaL is divided into a lower and an upper domain (Figure 3). The lower domain (residues 1−70) contains one helix (α1) and an antiparallel four-stranded β-sheet (β2−β1−β5−β6). The protein backbone after strand β2 continues outside the β-sheet and forms an additional two-stranded hairpin β-sheet (β3−β4). This two-stranded hairpin β-sheet is termed the lower lip of the active site, and on the basis of the refined thermal factors, it is the most flexible section within the folded protein−oligosaccharide complex. After strand β4, the backbone continues to become strand β5 of the four-stranded β-sheet. The upper domain of LaL (residues 71−154) is composed of five α-helices (α2−α6). Between helices α5 and α6, there is an 18-residue loop, part of which

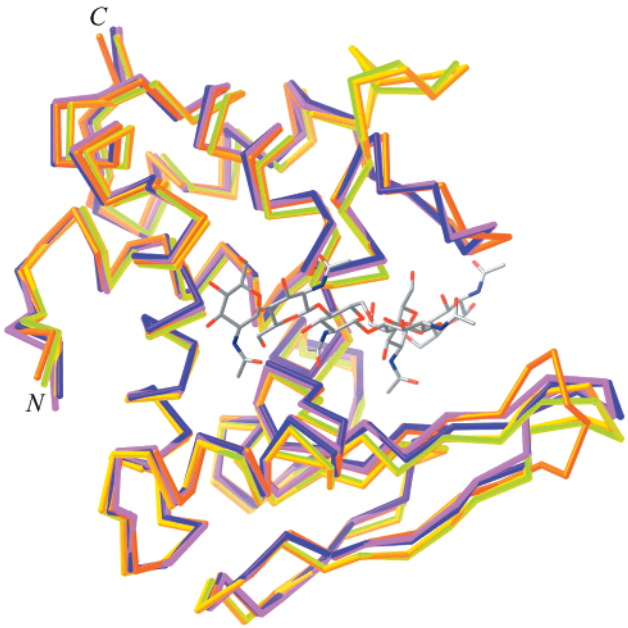

FIGURE 4: Structural comparison between LaL and mLaL. Shown are the least-squares superimposed Cα traces for the crystallographically independent A and B molecules of LaL in light and dark purple, respectively, and the crystallographically independent A−C molecules of mLaL in bright, medium, and dark yellow, respectively. Also shown are the six saccharide residues that bind to the LaL monomer. The orientation of the enzymes is slightly rotated around the vertical axis when compared to Figure 3 so as to highlight the different conformations of the upper lip in the LaL and mLaL monomers. This figure was produced using Ribbons (*54*).

covers the active site and is termed the upper lip (residues 127−139).

The active site of LaL is a deep elongated cleft located between the lower and upper domains. Traditionally, the active sites of lysozymes are divided into six subsites, A−F [or subsites −4 to 2, respectively, using the recently proposed nomenclature (*49*) for sugar-binding subsites in glycosylhydrolases]. In the LaL·$(GlcNAc)_6$ complex, each of these six subsites is occupied by one GlcNAc unit. Four GlcNAc units from one hexasaccharide bind to subsites A−D (subsites −4 to −1, respectively), while two GlcNAc units from another hexasaccharide occupy subsites E and F (subsites 1 and 2, respectively) (see below).

Comparison between the LaL·$(GlcNAc)_6$ Complex and mLaL. The structure of mLaL determined by Evrard and coworkers contains three molecules per asymmetric unit (*30*), while the structure presented here provides two crystallographically independent views of the LaL−oligosaccharide complex. As shown in Figure 4, the differences between the LaL·$(GlcNAc)_6$ complex and mLaL are concentrated in an area adjacent to where in the LaL·$(GlcNAc)_6$ complex the saccharide is located. Therefore, it can be concluded that the replacement of tryptophan residues with 7-azatryptophan does not affect the fold of LaL and that differences between the LaL·$(GlcNAc)_6$ complex and mLaL reflect differences caused by substrate binding.

The principal difference between the empty enzyme and the substrate complex is the conformation of the upper lip (excluding the upper lip, the rmsd between LaL and mLaL molecules is ∼0.9 Å, using 564 main chain atoms in the calculation). In molecules mLaL-A and -C, the conformation of the upper lip is such that the active site of the enzyme is wide open. In comparison, residues 127−139 in the LaL·$(GlcNAc)_6$ complex have moved toward the active site of the enzyme, thereby partially covering the bound substrate. The shift made by the tip of the upper lip is approximately 12 Å, and the rmsd for the main chain atoms of the upper lip is on the order of 7.7 Å (using 52 atoms in the calculation).

Intriguingly, enzyme molecule B in the mLaL structure possesses an upper lip loop conformation which is very similar to that of the substrate-bound conformation [rmsd of ∼1.4 Å between mLaL-B and the LaL-A/B·$(GlcNAc)_6$ complex for residues 127−139]. This observation may suggest that in the absence of bound substrate the upper lip is highly mobile and can occupy several conformations, one of them resembling the substrate-bound conformation. However, when the substrate binds, the degrees of freedom for this polypeptide segment are dramatically reduced, resulting in the single conformation seen in the two crystallographically independent LaL·$(GlcNAc)_6$ complexes. Alternatively, it is also possible that the upper lip conformation seen in mLaL-B is an artifact produced by crystal packing and that under physiological conditions this loop region is positioned such that the active site is always able to accept a substrate.

Interactions of the N-Acetylglucosamine Hexamer with LaL. Each *N*-acetylglucosamine hexamer $(GlcNAc)_6$ is straddled between two LaL molecules in the crystal structure, having four of its saccharide units bound to one enzyme molecule, and the remaining two units bound to a noncrystallographically related neighboring LaL molecule. From the perspective of the LaL enzyme, four of its six subsites (A−D) are occupied by four units of one *N*-acetylglucosamine hexamer, and subsites E and F are utilized by two units of a noncrystallographically related *N*-acetylglucosamine hexamer. Intriguingly, when comparing the H-bond and van der Waals interactions between the saccharide and enzyme in the two crystallographically independent LaL molecules, we observed that they are similar, but not identical. Figure 5 and Table 2 provide a comprehensive overview of saccharide−enzyme interactions as seen in the crystal structure, and some of these interactions will be highlighted below.

As expected, the *N*-acetylglucosamine units located at the two extremities of the hexasaccharide binding site, i.e., $(GlcNAc)_A$ and $(GlcNAc)_F$, only form van der Waals interactions with the LaL enzyme. The indole ring of Trp73 makes stacking interactions with $(GlcNAc)_B$ and $(GlcNAc)_C$. In addition to the stacking interactions, $(GlcNAc)_C$ binds to subsite C with a characteristic hydrogen bonding network between its 2-acetamido group and the backbone segments of LaL, an interaction common to most lysozyme structures (*48*). This typical hydrogen bonding network involves the main chain atoms of the protein acting like a clamp to interact with the 2-acetamido group from opposite sides. In LaL, the oxygen atom of the 2-acetamido hydrogen bonds with the amino group in Leu70 while the nitrogen atom of the 2-acetamido interacts with the carbonyl oxygen in Ile123 (Figure 5).

Ligand-binding modes in subsites D and E have elicited the most interest in lysozyme research since the catalysis of the cleavage of the $\beta(1\rightarrow4)$ glycosidic bond occurs between these subsites. As discussed above, in the LaL·$(GlcNAc)_6$

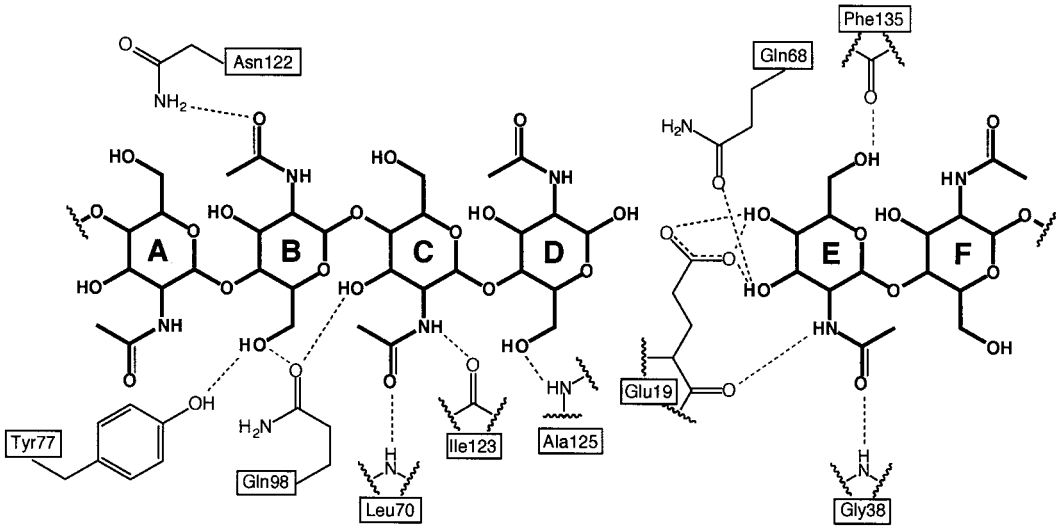

FIGURE 5: Schematic overview of all the interactions observed between the active site of LaL and the hexa-*N*-acetylchitohexaose. Only rings A−D of one hexasaccharide and rings E and F of the second hexasaccharide are shown. Dashed lines are used to indicate hydrogen bond interactions (see also Table 2).

Table 2: Saccharide−Protein Hydrogen Bond Interactions

subsite	saccharide−protein H-bond	molecule A (Å)	molecule B (Å)
A	none	−	−
B	O6−Gln98 OE1	−	2.8
	O6−Tyr77 OH	2.8	3.0
	O7−Asn122 ND2	2.8	3.0
C	N2−Ile123 O	2.9	2.7
	O3−Gln98 OE1	3.0	2.8
	O7−Leu70 N	3.3	3.4
D	O6−Ala125 N	2.6	2.7
E	N2−Glu19 O	2.9	2.9
	O3−Glu19 OE1	−	3.4
	O3−Gln68 OE1	3.0	2.7
	O4−Glu19 OE1	2.7	2.8
	O4−Glu19 OE2	3.4	3.3
	O6−Phe135 O	2.7	2.6
	O7−Gly38 N	3.0	2.8
F	none	−	−

crystal structure, the saccharide units occupying subsites D and E belong to two different hexamers, thus creating an intrinsic break between the GlcNAc residues in subsites D and E. $(GlcNAc)_D$ is unlikely to be positioned in a catalytically competent conformation since it does not interact with the catalytic acid, Glu19. Also, a catalytically competent conformation would imply distortion of the $(GlcNAc)_D$ residue; i.e., the 6-OH group must be positioned such that transglycosylation can occur. However, $(GlcNAc)_D$ forms a unique stacking interaction with Tyr132, which is in turn hydrogen bonded to the carbonyl oxygen of Asn122.

Interestingly, $(GlcNAc)_E$ is buried deep in the active site crevice and forms numerous interactions with the enzyme. In fact, the extent of interaction of $(GlcNAc)_E$ with LaL is comparable to that of $(GlcNAc)_C$, which has been observed in other lysozyme structures to have the most interactions with the protein (*48*). Indeed, the catalytic acid, Glu19, is within hydrogen bonding distance of the glycosidic oxygen, O4, of $(GlcNAc)_E$ in monomer B.

DISCUSSION

LaL−Oligosaccharide Binding. Difficulties in the preparation of suitably diffracting crystals of wild-type LaL have been noted by Evrard and co-workers, and led to the finding that the replacement of Trp residues with 7-azatryptophan residues in this protein allowed for the formation of suitably diffracting crystals (*30*, *31*). It has been suggested that the incorporation of this unnatural amino acid may have resulted in additional hydrogen bonding interactions that could have contributed to the formation of these crystals (*31*). In our own hands, many attempts to produce suitably diffracting crystals of the wild-type LaL also met with failure. We previously noted the ability of chitin oligosaccharides to bind to LaL as observed by NMR and calorimetry experiments (*33*, *34*, *44*). However, these oligosaccharides were unable to serve as substrates, unlike for lysozymes such as HEWL (*1*). The formation of complexes between LaL and chitin oligosaccharides was further investigated by following changes in the intrinsic fluorescence properties of LaL (data not shown). LaL was found to fluoresce under 280 nm excitation with an emission maximum at 343−345 nm at pH 7.0. A progressive decrease in the emission maximum (λ_{max}) that depended upon oligosaccharide length and concentration was observed. Whereas $(GlcNAc)_2$ caused no change in λ_{max} or fluorescence intensity, and $(GlcNAc)_3$ produced only a marginal blue shift, increasing concentrations of $(GlcNAc)_4$, $(GlcNAc)_5$, and $(GlcNAc)_6$ decreased λ_{max} from ∼345 nm (in the absence of saccharide) to ∼337 nm in their presence. Fluorescence intensity was also observed to increase. Maltotetraose, which has been previously shown not to bind to the enzyme by NMR and calorimetry, produced no fluorescence emission shifts or changes in intensity (*33*). The blue shift suggests that the environment surrounding the Trp residues that dominate the fluorescence of LaL decreases in polarity upon oligosaccharide binding. A similar effect is seen with oligosaccharide binding to HEWL and indicates a similar interaction between tryptophan residues of LaL and an oligosaccharide may also be occurring. We also found that oligosaccharides wherein $n \geq 4$ in $(GlcNAc)_n$ are able to protect LaL from carbodiimide inactivation (likely due to carboxyl group modification), indicating that the oligosaccharide is likely protecting an active site glutamate/aspartate from chemical modification (Figure 3). Using the observations that $(GlcNAc)_4$ and longer

oligosaccharides appear to interact directly with the active site in a substantial way, attempts to produce suitable crystals of a LaL−oligosaccharide complex were carried out from which the LaL·$(GlcNAc)_6$ structure was finally determined. This has allowed for an analysis of both global and local conformational alterations occurring upon saccharide binding. In addition, a comparison of the structures of LaL with the lytic transglycosylases from *E. coli* complexed with saccharides is now possible, and thus, an examination of what structural features differentiate lytic transglycosylases from other lysozymes can now be performed.

Transglycosylation Reaction Mechanism; Role of Subsite E and the Absence of Catalytic Asp. Despite the vast number of lysozyme structures available to date, saccharide interactions in subsites E and F have not been seen crystallographically (*48*, *50*, *51*) except for recent studies on the lytic transglycosylases Slt35 and Slt70 (*28*, *29*). For example, although six saccharides are observed in a human lysozyme structure (PDB entry 1LZS), the $(GlcNAc)_6$ was in fact cleaved during crystallization into $(GlcNAc)_4$ and $(GlcNAc)_2$. The disaccharide does not bind directly to subsites E and F, as it is located too far from the catalytic Glu, but rather it is trapped near these sites (*32*). The present LaL·$(GlcNAc)_6$ complex indicates how saccharide residues from peptidoglycan interact at subsites E and F after a cleavage reaction.

The fact that there are no other lysozyme structures in which subsites E and F are filled could indicate that in these other lysozymes, the saccharide residues at positions E and F do not interact with the protein very strongly. The weak interaction allows the saccharides to diffuse away quickly from the E and F subsites after cleavage so that a water molecule can diffuse into the active site and attack the C1 atom of the oxocarbonium ion intermediate, thus completing the regular hydrolysis reaction. The unusual stable binding of $(GlcNAc)_E$ in LaL points to the possibility that the saccharide residues tend to stay in the active site longer than in other lysozymes so that water molecules are prevented from attacking the oxocarbonium ion, allowing tranglycosylation with a 6-OH group to occur rather than hydrolysis.

According to the generally accepted lysozyme mechanism, the first step of catalysis generates an oxocarbonium ion intermediate, which adopts a high-energy half-chair conformation (*1*). The intermediate is stabilized by extensive interactions with the protein. It has been proposed for HEWL that important stabilization of the oxocarbonium ion is contributed by the proximity of an ionized negatively charged Asp52. Counterparts to Asp52 have been located in other types of lysozymes. However, in these lysozymes, mutation of the equivalent Asp52 seems to have a less deleterious effect than the equivalent catalytic Glu (*52*). In fact, the corresponding Asp52 residue is absent in goose egg white lysozyme (GEWL) (*53*). LaL is similar to GEWL in that it has no Asp52 counterpart. Previous suggestions that Asp34 may play a role in LaL equivalent to that of Asp52 in HEWL, that is of a negatively charged side chain that stabilizes the developing oxocarbonium ion in the transition state, seem unfounded as the crystal structure of mLaL or the LaL·$(GlcNAc)_6$ complex indicates that Asp34 is not proximal to the D and E subsites (*47*). The structure of the LaL·$(GlcNAc)_6$ complex is important in this regard, as it could be argued that ligand binding might cause conformational changes in LaL which place Asp34 in the appropriate position for catalysis. On the basis of the structure of the LaL·$(GlcNAc)_6$ complex, this is obviously not the case. Furthermore, no other Asp or Glu residues are within 10 Å of Glu19 in the saccharide-bound state of LaL. A hydrogen bond between the hydroxyl of Ser126 and Glu19, seen in mLaL, is still present in the saccharide complex of LaL and may aid in the protonation event initiated by Glu19 and subsequent proton transfers in the latter steps in the enzyme mechanism, including 6-OH attack on the developing oxocarbonium ion. LaL therefore joins the goose lysozyme as well as the *E. coli* lytic transglycosylases in not requiring a second Glu/Asp residue for enzyme activity. Note that from a mechanistic viewpoint the absence of a second Glu/Asp residue is reasonable. Since immediately after cleavage subsite E remains occupied thereby precluding a water molecule from entering the active site, the 6-OH group from the muramic acid that is undergoing the enzymatic cleavage provides the incoming alcohol function by necessity, thus resulting in transglycosylation.

Comparison to Other Lysozymes. A structural comparison between LaL and c- and v-type lysozymes (i.e., HEWL and T4 lysozyme) has previously been presented (*30*). Here we will direct the attention to the comparison between LaL and the more closely related bacterial lytic transglycosylases and how they as a group differ from other lysozymes. In addition to the LaL enzyme presented here, crystal structures are available for two other lytic transglycosylases, Slt70 and a proteolytic fragment of MltB designated Slt35 (*26*−*29*). Of these three lytic transglycosylases, LaL is by far the smallest (17.8 kDa vs 36 and 70 kDa for MltB and Slt70, respectively), which can be rationalized by noting that MltB and Slt70 are involved in peptidoglycan renovation and thus require stringent enzymatic regulation, i.e., additional domains, while LaL's mandate is to simply lyse the bacterial cell. Focusing on the catalytic domains of Slt70 and MltB (i.e., Slt35), we observed clear similarity between their folds and that of LaL, specifically in the core. Much of this similarity is not unique to the lytic transglycosylases, but defines a common lysozyme scaffold (*30*). However, a helix located beneath subsites A−D (helix α2 in LaL) appears to be unique to the lytic transglycosylase family of enzymes, based on the current three-dimensional structural database.

As stated above, the functional commonality among lytic transglycosylases that makes them distinct from other lysozymes is the particular cleavage reaction of peptidoglycan resulting in the generation of 1,6-anhydromuramic acid terminal residues. Such a cleavage reaction by necessity imposes constraints on the structure of lysozyme-like lytic transglycosylases. Specifically, two constraints must be met: (a) water must be prevented from approaching the site of cleavage so as to avoid a hydrolysis reaction, and (b) the saccharide in subsite D must undergo a greater distortion compared to other lysozymes so as to allow the C6 hydroxyl group to attack C1. In addition, our results also suggest that the absence of the second catalytic base is at least a facilitating feature. A naïve conclusion would be to assume that the two structural constraints imposed by the reaction are met by a common architectural feature, that being that the helix located beneath subsites A−D uniquely observed in the lytic transglycosylases is primarily responsible for the

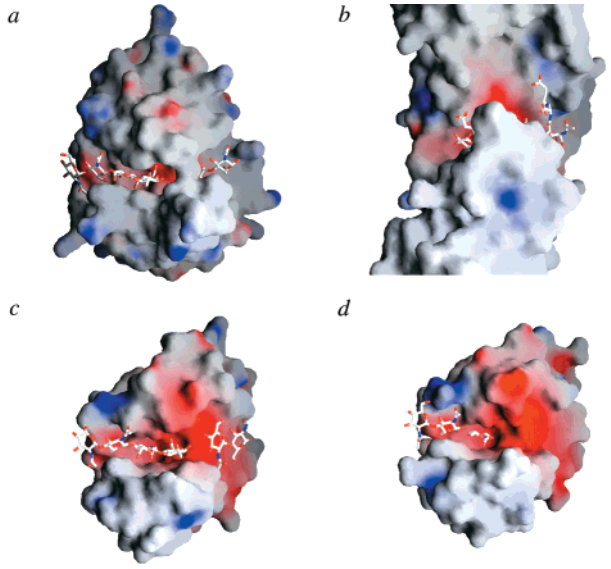

FIGURE 6: Surface depictions of the active site of four lysozymes. Shown in panel a is LaL in complex with two hexa-*N*-acetylchitohexaose molecules (only saccharide moieties bound to saccharide subsites in LaL are displayed). Panel b displays Slt35 in complex with two muropeptides (PDB entry 1D0K). Panel c presents human lysozyme in complex with cleaved hexa-*N*-acetylchitohexaose (PDB entry 1LZS). Panel d shows HEWL in complex with tri-*N*-acetylchitotriose (PDB entry 1HEW). The coloring of the surface is according to electrostatic potential, ranging from −50 to 50 k_bT (red to blue, respectively). This figure was generated using the program Grasp (*55*).

specific peptidoglycan cleavage reaction performed by these enzymes. However, we are unable to convincingly link this specific structural commonality to the transglycosylation reaction mechanism.

Our analysis of LaL suggests that stronger saccharide binding in subsite E is the mechanism by which this enzyme may prevent a water molecule from completing the hydrolysis reaction. In fact, this has also been suggested from the structures of saccharide−Slt complexes (*28*, *29*) (see below). Intriguingly, the structural reason for the apparent stronger affinity of the E subsite for the saccharide in LaL and other transglycosylases than for lysozyme enzymes is not immediately clear. As can be seen from Table 2 and Figure 5, the main hydrogen bond interactions between the saccharide and the E subsite are made by Glu19 and Gln68, both of which are conserved among all lysozymes, and thus not unique to lytic transglycosylases. This suggests that van der Waals interactions must play a critical role in substrate binding to the E subsite. When analyzing the molecular surface of different lysozymes (see Figure 6), we can infer that the lytic transglycosylases do either form van der Waals interactions with the saccharide bound in subsite E or provide an obstruction which hinders diffusion from the E subsite. However, the method by which the E saccharide is kept in subsite E differs among lytic transglycosylases. In LaL, the lower lip and upper lip are responsible for covering the E subsite, while in Slt70 and Slt35, the additional non-lysozyme domains appear to restrict diffusion of a saccharide out of the E subsite. Furthermore, when comparing the upper and lower lips of LaL to those of other lysozymes, we could not identify specifically unique features. HEWL lacks the upper lip and GEWL the lower lip, but T4 lysozyme possess both an upper and lower lip that are analogous to those of LaL.

With respect to achieving a greater distortion of the saccharide in subsite D in lysozyme-like lytic transglycosylases so as to allow the formation of the 1,6-anhydro linkage, again it proves to be difficult to pinpoint a unique lytic transglycosylase feature which can be considered responsible for this task. On the basis of this, it can be argued that perhaps saccharide distortion is not a limiting factor, but that all lysozymes provide sufficient distortion of the saccharide residing in subsite D. If this is the case, then the combination of the absence of a catalytic Asp and the exclusion of water from the active site is sufficient to promote a transglycosylation instead of a hydrolysis reaction.

CONCLUSIONS

Despite the well-known area of lysozyme biochemistry, nature continually presents new perspectives on this area of biochemistry. In the current structural study, a lysozyme is observed in which all six subites are fully occupied and the detailed interactions between the saccharide and the enzyme are available. Although smaller in size, several similarities exist between LaL and the bacterial lytic transglycosylases. First, the overall fold appears to be similar with a specific helix present in LaL and Slt35 and -70. Second, only one catalytic acidic residue is present in the active site of these enzymes. The lack of a requirement for the presence of a second Asp residue in these enzymes also appears to coincide with evidence for the tighter binding of the E sugar to the active site. This more stable interaction may block competing water attack on the oxocarbonium intermediate, allowing the 6-OH of the D subsite muramic acid to form the 1,6-anhydro linkage. Comparison of our results with structural studies of other lysozymes suggests that the structural features that primarily differentiate lytic transglycosylases and other lysozymes are a combination of (a) obstruction of subsite E so that diffusion of the saccharide away from this location is hindered and (b) removal of the second catalytic acid.

ACKNOWLEDGMENT

We thank past and present members of the Berghuis and Honek labs for their assistance. We also thank the MacCHESS people for their assistance during the collection of data sets at the CHESS F2 beamline, which unfortunately did not prove to be useful.

REFERENCES

1. Jollès, P. (1996) *Lysozymes: Model enzymes in biochemistry and biology*, Vol. 75, Birkhäuser Verlag, Basel, Switzerland.
2. Shockman, G. D., and Holtje, J.-V. (1994) *Bacterial Cell Wall*, Vol. 27, Elsevier Science B. V., Amsterdam.
3. Campbell, A. (1961) *Virology 14*, 22−32.
4. Black, L. W., and Hogness, D. S. (1969) *J. Biol. Chem. 244*, 1982−1987.
5. Bienkowska-Szewczyk, K., Lipinska, B., and Taylor, A. (1981) *Mol. Gen. Genet. 184*, 111−114.
6. Taylor, A., Das, B. C., and Van Heijenoort, J. (1975) *Eur. J. Biochem. 53*, 47−54.
7. Holtje, J. V., Mirelman, D., Sharon, N., and Schwarz, U. (1975) *J. Bacteriol. 124*, 1067−1076.
8. Engel, H., Kazemier, B., and Keck, W. (1991) *J. Bacteriol. 173*, 6773−6782.
9. Engel, H., van Leeuwen, A., Dijkstra, A., and Keck, W. (1992) *Appl. Microbiol. Biotechnol. 37*, 772−783.
10. Ursinus, A., and Holtje, J. V. (1994) *J. Bacteriol. 176*, 338−343.

11. Dijkstra, A. J., Hermann, F., and Keck, W. (1995) *FEBS Lett. 366*, 115−118.
12. Ehlert, K., Holtje, J. V., and Templin, M. F. (1995) *Mol. Microbiol. 16*, 761−768.
13. Lommatzsch, J., Templin, M. F., Kraft, A. R., Vollmer, W., and Holtje, J. V. (1997) *J. Bacteriol. 179*, 5465−5470.
14. Kraft, A. R., Templin, M. F., and Holtje, J. V. (1998) *J. Bacteriol. 180*, 3441−3447.
15. Koonin, E. V., and Rudd, K. E. (1994) *Trends Biochem. Sci. 19*, 106−107.
16. Dijkstra, A. J., and Keck, W. (1996) *J. Bacteriol. 178*, 5555−5562.
17. Holtje, J. V. (1998) *Microbiol. Mol. Biol. Rev. 62*, 181−203.
18. Luker, K. E., Collier, J. L., Kolodziej, E. W., Marshall, G. R., and Goldman, W. E. (1993) *Proc. Natl. Acad. Sci. U.S.A. 90*, 2365−2369.
19. Martin, S. A., Karnovsky, M. L., Krueger, J. M., Pappenheimer, J. R., and Biemann, K. (1984) *J. Biol. Chem. 259*, 12652−12658.
20. Johannsen, L. (1993) *APMIS 101*, 337−344.
21. Fleming, T. J., Wallsmith, D. E., and Rosenthal, R. S. (1986) *Infect. Immun. 52*, 600−608.
22. Krueger, J. M., Karnovsky, M. L., Martin, S. A., Pappenheimer, J. R., Walter, J., and Biemann, K. (1984) *J. Biol. Chem. 259*, 12659−12662.
23. Dokter, W. H., Dijkstra, A. J., Koopmans, S. B., Stulp, B. K., Keck, W., Halie, M. R., and Vellenga, E. (1994) *J. Biol. Chem. 269*, 4201−4206.
24. Dokter, W. H., Dijkstra, A. J., Koopmans, S. B., Mulder, A. B., Stulp, B. K., Halie, M. R., Keck, W., and Vellenga, E. (1994) *Infect. Immun. 62*, 2953−2957.
25. Biberstine, K. J., and Rosenthal, R. S. (1994) *Infect. Immun. 62*, 3276−3281.
26. Thunnissen, A. M., Dijkstra, A. J., Kalk, K. H., Rozeboom, H. J., Engel, H., Keck, W., and Dijkstra, B. W. (1994) *Nature 367*, 750−753.
27. van Asselt, E. J., Dijkstra, A. J., Kalk, K. H., Takacs, B., Keck, W., and Dijkstra, B. W. (1999) *Struct. Folding Des. 7*, 1167−1180.
28. van Asselt, E. J., Thunnissen, A. M., and Dijkstra, B. W. (1999) *J. Mol. Biol. 291*, 877−898.
29. van Asselt, E. J., Kalk, K. H., and Dijkstra, B. W. (2000) *Biochemistry 39*, 1924−1934.
30. Evrard, C., Fastrez, J., and Declercq, J. P. (1998) *J. Mol. Biol. 276*, 151−164.
31. Evrard, C., Fastrez, J., and Declercq, J. P. (1999) *Acta Crystallogr. D55*, 430−435.
32. Song, H., Inaka, K., Maenaka, K., and Matsushima, M. (1994) *J. Mol. Biol. 244*, 522−540.
33. Duewel, H. S., Daub, E., and Honek, J. F. (1995) *Biochim. Biophys. Acta 1247*, 149−158.
34. Duewel, H., Daub, E., Robinson, V., and Honek, J. F. (1997) *Biochemistry 36*, 3404−3416.
35. McPherson, A. (1990) *Eur. J. Biochem. 189*, 1−23.
36. Jancarik, J., and Kim, S.-H. (1991) *J. Appl. Crystallogr. 24*, 409−411.
37. Otwinowski, Z., and Minor, W. (1997) *Methods Enzymol. 276*, 307−326.
38. Matthews, B. W. (1968) *J. Mol. Biol. 33*, 491−497.
39. Brünger, A. T. (1992) *X-PLOR: A system for crystallography and NMR*, version 3.1, Yale University Press, New Haven, CT.
40. Jones, T. A., and Kjeldgaard, M. (1993) *O*, version 5.9, Department of Molecular Biology, Uppsala University, Uppsala, Sweden.
41. Read, R. J. (1986) *Acta Crystallogr. A42*, 140−149.
42. Kleywegt, G. J., and Brünger, A. T. (1996) *Structure 4*, 897−904.
43. Laskowski, R. A., MacArthur, M. W., Moss, D. S., and Thornton, J. M. (1993) *J. Appl. Crystallogr. 26*, 283−291.
44. Vaughan, M. D., Cleve, P., Robinson, V., Duewel, H. S., and Honek, J. F. (1999) *J. Am. Chem. Soc. 121*, 8475−8478.
45. Lundblad, R. L. (1991) *Chemical Reagents for Protein Modification*, 2nd ed., CRC Press, Boca Raton, FL.
46. Levy, H. M., Leber, P. D., and Ryan, E. M. (1963) *J. Biol. Chem. 238*, 3654−3659.
47. Jespers, L., Sonveaux, E., and Fastrez, J. (1992) *J. Mol. Biol. 228*, 529−538.
48. Strynadka, N. C., and James, M. N. (1996) in *Lysozymes: Model Enzymes in Biochemistry and Biology* (Jollès, P., Ed.) pp 185−222, Birkhäuser Verlag, Basel, Switzerland.
49. Davies, G. J., Wilson, K. S., and Henrissat, B. (1997) *Biochem. J. 321*, 557−559.
50. Vollan, V. B., Hough, E., and Karlsen, S. (1999) *Acta Crystallogr. D55*, 60−66.
51. Muraki, M., Harata, K., Sugita, N., and Sato, K. (1998) *Acta Crystallogr. D54*, 834−843.
52. Matsumura, I., and Kirsch, J. F. (1996) *Biochemistry 35*, 1881−1889.
53. Weaver, L. H., Grutter, M. G., and Matthews, B. W. (1995) *J. Mol. Biol. 245*, 54−68.
54. Carson, M. (1997) *Methods Enzymol. 277*, 493−505.
55. Nicholls, A., Sharp, K. A., and Honig, B. (1991) *Proteins: Struct., Funct., Genet. 11*, 281−296.

BI0028035